

Graphitic andesite tuffs resulting from high-Mg tholeiite and sediment interaction; Nûgssuaq, West Greenland

ASGER KEN PEDERSEN



Pedersen, A. K.: Graphitic andesite tuffs resulting from high-Mg tholeiite and sediment interaction; Nûgssuaq, West Greenland. *Bull. geol. Soc. Denmark*, vol. 27, Special Issue, pp. 117–130, Copenhagen, July 30th, 1978. <https://doi.org/10.37570/bgSD-1978-SI-13>

Tuffs from the Agatdal Formation of Nûgssuaq show a dominance of olivine-graphite-andesites and orthopyroxene-graphite-andesites while rock types similar to the overlying tholeiite basalts of the Vaigat Formation are subordinate. The tuffs were formed when highly magnesian tholeiitic picrite melts were emplaced into high-level magma chambers within carbon-rich sedimentary strata. Explosive reactions were triggered after extensive reactions with the sediments. Glass grains are well preserved and some tuffs still contain quenched high-temperature sulphide blebs with metallic iron. Due to the high magnesium content the graphite-andesites are very unusual magma types and can be compared to some native iron bearing intermediate lavas from the Vaigat Formation of northern Disko thought to have erupted largely contemporaneously after having evolved through similar processes.

Asger Ken Pedersen, Geologisk Museum, Øster Voldgade 5–7, DK-1350 Copenhagen K, Denmark. March 1st, 1978.

The native iron found in Tertiary igneous rocks on the island of Disko in West Greenland has been famous since the early descriptions by Norden-skiöld (1871) and Steenstrup (1875, 1882). While localities of native iron are numerous on Disko (Steenstrup 1882) only two localities are known from the neighbouring Nûgssuaq peninsula despite a considerable similarity in sedimentary and volcanic lithology (see reviews by Henderson, Rosenkrantz & Schiener 1976 and Clarke & Pedersen 1976). Steenstrup (1882) found iron-bearing graphite-rich lava blocks in the scree slopes at Nûk qiterdleq on the south coast and White & Schuchert (1898) found an iron-bearing dolerite dyke later described by Phalen (1903) at Qaersut on the north coast (fig. 1). A new major occurrence of highly reduced volcanic rocks with native iron has now been found in the tuffs of the Abraham Member of the Agatdal Formation in central Nûgssuaq.

The tuffs from the Abraham Member (for stratigraphy see table 1 and Rosenkrantz in Koch (1959), Rosenkrantz (1970) and Henderson et al. (1976)) were formerly believed by Rosenkrantz (1951, 1955), Munck & Noe-Nygaard (1957) and Rosenkrantz & Pulvertaft (1969) to represent an initial phase of the volcanism, which eventually led to the build up of the West Greenland Basalt

Group. However, work by Koch (1959), Pedersen (1973) and Hald (1977) suggests that the tuffs are contemporary with the eruption of extensive lavas and hyaloclastites of the Vaigat Formation in

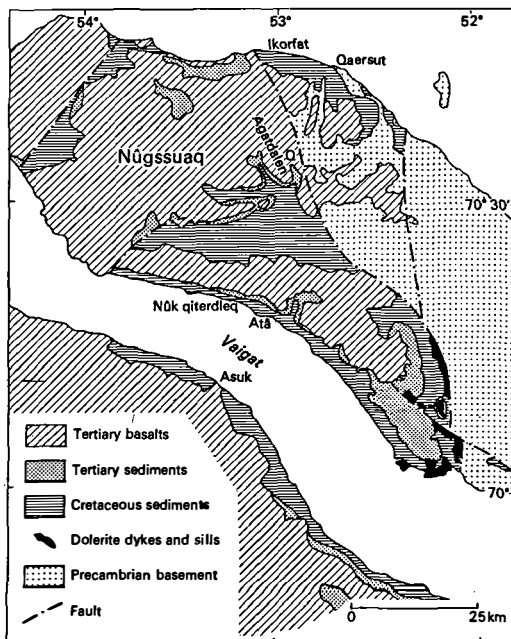


Fig. 1. Sketch map of central Nûgssuaq and northern Disko.

western Nûgssuaq and Disko. While non-volcanic marine and deltaic sediments were deposited in central and eastern Nûgssuaq and Disko, lavas and hyaloclastites gradually transgressed eastwards and eventually spread over the sedimentary basins.

The late Prof. A. Rosenkrantz sampled the Abraham Member tuff sequence at several localities in the Agatdal area for study by S. Munck who, on her retirement, left the material to me. The sample labels represent the only written record but from these a rough local stratigraphy has been constructed (table 1).

Geology of the tuffs

At the type locality in Turritlekløft, Agatdalen, the Abraham Member is 12 m thick and is composed of alternating black shales and rather coarse fossiliferous tuffs. Schematic profiles, photographs and brief lithological notes are given by Koch (1963), Hansen (1970), Rosenkrantz (1970), Floris (1972) and Henderson et al. (1976). The sedimentological and palaeontological evidence in-

dicates that the tuffs were deposited in saline shallow water transitional to deltaic facies. The Abraham Member overlies sandstones of the Andreas Member and is covered by picritic hyaloclastites from the Vaigat Formation. The tuffs are found within an area of a few hundred square kilometres around Agatdalen-Qaersutjægerdalen, but due to poor exposures and the lack of detailed mapping the areal distribution is unknown.

The following general notes are based on samples from Turritlekløft in Agatdalen (table 1). Eight major tuff horizons have been recognized by A. Rosenkrantz. They vary in thickness from below 10 to 50 cm. Below the lowermost major horizon several thin tuffs are found, and between the major layers there are numerous thin tuffs. The major tuff horizons have a cumulative thickness of about 2.5 m, and together with the minor tuff layers they probably account for about 25 per cent of the deposits of the Abraham Member. The maximum size of the volcanic fragments varies from layer to layer from about 0.5 to 7 mm. Combining evidence from petrography, fragment size and layer thickness it is concluded that in general the eruption sites were within a few tens of kilometres from Agatdalen.

In most cases a shale layer separates individual tuff layers, and it can be concluded that the tuffs of the Abraham Member provide a volcanic multievent record.

Table 1. Schematic section through the Abraham Member tuffs at Turritlekløft, Agatdalen.

Stratigraphic unit	Main tuff horizon no.	Thickness in mm	Maximum size of volcanic fragments in mm	Dominant volcanic rock type
Vaigat Formation				Picrite basalt
Agatdal Formation Abraham Member	8	400	1.5	Graphite-andesite with opx
	7	150	0.7	Graphite-andesite with ol + opx
	6	500	1	Graphite-andesite with ol
	Between 5 and 6. Minor horizon 2 from above	80	1.5	Graphite-andesite with ol + opx
	5	200	3	Graphite-andesite with opx
	4	200	2	Graphite-andesite with opx
	3	200	1.5	Graphite-andesite with opx
	2*	300	0.5	Tholeiitic basalt with plag + cpx
	2	350	4	Graphite-andesite with ol + opx
	1	?	7	Graphite-andesite with ol + opx
30 cm below 1	>40	1	Graphite-andesite with opx	
Andreas Member				

* This tuff appears as the main tuff horizon 2 in Qaersutjægerdalen.

State of preservation of the tuffs

The tuffs may have been subject to chemical and mineralogical modifications in three main stages, (a) recent weathering, (b) regional metamorphism and metasomatism and (c) pre-diagenesis alteration and diagenesis.

(a) recent weathering

A number of samples are hard non-porous cemented rocks. These are generally unaffected by recent weathering, while weakly or non-cemented samples, which constitute the bulk of the material, form crumbly strongly weathered masses. Some of this weathering may be of early Tertiary age. However, even in such masses glass cores may be preserved in some grains, and most pyroxene phenocrysts are still fresh. Most of the non-cemented

samples have been altered to palagonite and clay and other sheet silicates. Even in these rocks the volcanic grain boundaries and textures can still be distinguished, enabling identification of the dominant volcanic rock types present.

(b) regional metamorphism and metasomatism

The tuffs of the Abraham Member are covered by more than a kilometre of hyaloclastites and lavas which have suffered widespread alteration through circulating hot water, resulting in the formation of zeolites, Ca-hydrosilicates and sheet silicates. Tuff horizons within these volcanic rocks are mostly extensively altered. In contrast, no trace of such hot water alteration can be found in the underlying tuffs of the Abraham Member. Zeolites are absent or, if present, very scarce; instead there are subordinate silica precipitates. It can be concluded petrographically that the tuffs are virtually unmetamorphosed. In agreement with this E.J. Schiener (pers. comm. 1976) has observed from coal petrography that the organic components in the sediments of the Agatdal Formation in this area have never been heated above 55°C.



Fig. 2. Yellow basaltic glass with chromite crystals and a carbonate pseudomorph after olivine. Note the colourless palagonite formed along the margins and along cracks in the glass. GGU 8542.

(c) pre-diagenesis alteration and diagenesis

Apart from possible early weathering two types of early alteration have been observed. First, a characteristic rim of colourless isotropic palagonite is found around and along cracks in yellow basaltic glass grains in many samples (fig. 2). In several tuffs this rim has a fairly constant thickness of about 12 microns. Table 2 shows the chemical composition of the fresh yellow basaltic glass compared with that of the colourless rims. The colourless rims are hydrated (low totals) and have suffered loss of the basic oxides FeO, MgO and CaO, while an enrichment in K₂O has taken place. The considerable loss of iron is unusual and is attributed to a reducing local environment in the graphite-rich tuffs which may have prevented oxidation to the less soluble ferric iron. Apart from the iron the chemical pattern of change is similar to that observed when Mid-Ocean-Ridge-Basalt (MORB) glasses are altered on the sea floor, e.g. Thompson (1973), Hart, Erlank & Kable (1974) and Scarfe & Smith (1977). It is concluded that the colourless palagonite rims resulted from an initial exposure to saline water. Although the Abraham Member glasses were exposed to seawater in a near-shore environment (lower P_{H₂O}) and at different temperatures (higher), a qualitative exposure-time estimate of 3000–4000 years can be obtained from the data of Hekinian & Hoffert

Table 2. Chemical analyses illustrating the alteration processes.

	1		2		3		4		5	
No. of analyses	4	std †	1	1	1	1	1	1	1	
SiO ₂	48.55	0.23	58.85	52.42	48.57	45.30				
TiO ₂	1.41	0.06	1.84	1.00	0.86	0.83				
Al ₂ O ₃	15.03	0.14	18.08	14.93	15.16	13.33				
FeO*	10.39	0.12	0.36	12.09	16.55	20.22				
MgO	8.40	0.13	0.81	7.44	5.96	6.62				
CaO	12.76	0.08	2.58	8.43	7.99	7.65				
Na ₂ O	2.13	0.12	2.41	2.05	2.07	1.79				
K ₂ O	0.19	0.04	0.95	0.67	0.62	0.58				
	98.86		85.88	99.03	97.78	96.32				
Mg/(Mg + Fe _{total})	0.59		0.80	0.52	0.39	0.37				

* Total iron as FeO † One standard deviation

1: Yellow glass with plagioclase microphenocrysts. GGU 8542.

2: Colourless palagonite rim on glass of analysis 1.

3: Yellow basaltic glass, sediment contaminated, unaltered.

GGU 5646, tuff layer 1.

4: Dark brown core of coloured spherical glass grain.

GGU 5646, tuff layer 1.

5: Black glass margin of same grain as analysis 4.

(1975), using their observed palagonite growth rate estimate of 3.5 microns per 1000 years on MORB glasses. This is considered to represent the time from eruption to the chemical sealing of the sediment system.

The second type of alteration has only been observed in sample GGU 5646, tuff layer no. 1, where glass grains in the upper part of the tuff have been abraded to spherical bodies. Many of these grains become increasingly dark-coloured outwards and may be opaque at the margins. The chemical composition of a strongly colour-zoned glass and of an opaque sphere is compared with an unaltered glass from the same tuff table 2 (analyses 4-5). The dominant effect of this alteration is a strong increase in the total iron content while hydration is moderate. The alteration probably took place under oxidizing conditions when parts of the ash were being reworked prior to the final deposition. In the same sample a tuff 2 mm above layer no. 1 is unaffected by this alteration.

A general alteration affected most samples, probably during the diagenetic stage: with the exception of olivine microphenocrysts in some glassy andesites, olivines have been altered to carbonates or green sheet silicates, while a carbonate-impregnation and formation of clay and palagonite substances affected a number of tuffs.

Petrography of the volcanic rocks

The predominant volcanic rock in the tuffs is graphite-andesite with phenocrysts of orthopyroxene and/or olivine (table 1). In addition tholeiitic basalts are found with varying amounts of pseudomorphed olivine, plagioclase, chromite and rare augite. Descriptions of three selected samples (of which one is composed of several individual tuff layers) cover the range of magma types occurring in the tuffs.

Silicates, oxides and glasses

Sample GGU 5646 from an unspecified position in Agatkløft is the most complex and informative specimen (fig. 3). The sample is 6 cm thick with nine individual ash layers separated by shale, the whole carbonate cemented. The most homogeneous are tuff layers 2 and 3, each of which is only a few millimetres thick. They are composed of clear yellow basaltic glass which often carries euhedral plagioclase phenocrysts ($An_{76}-An_{80}$) (fig. 4). The glass (table 3 no. 2) is an only slightly hydrated and homogeneous tholeiitic basalt.

Tuff layer 1 is about 20 mm thick and contains a large range of

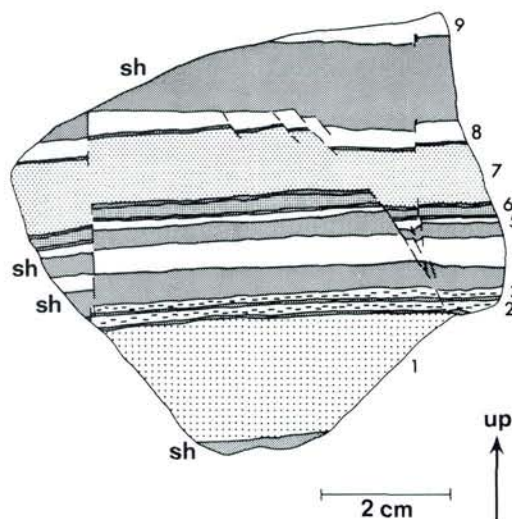


Fig. 3. Sketch of a section cut through sample GGU 5646 from Agatkløft. Nine individual ash falls (indicated by numbers) separated by shale layers (sh) are recorded in this rock, which became fractured prior to extensive carbonate-impregnation. Tuff layers mentioned in the text are stippled, the others are light grey. Shale sediments are dark grey.

glass compositions with abraded and altered grains. The volcanic grains vary in crystallinity, some are entirely crystalline but most are glasses with or without phenocrysts or xenocrysts. All the analysed glasses show evidence of reaction with sediments at high temperatures. The least modified are yellow basaltic grains (table 3 no. 3) some of which carry native iron. The grains are

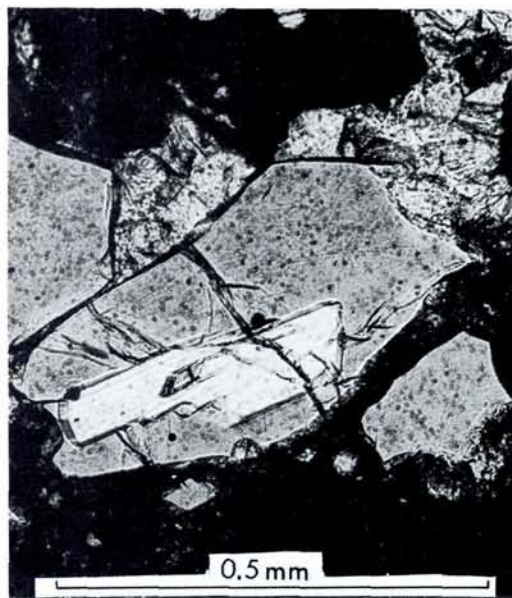


Fig. 4. Yellow basaltic glass with euhedral phenocrysts of plagioclase. Note radiating masses of carbonate and opaque matrix. GGU 5646, tuff layer no. 1.

Table 3. Chemical analyses of fresh natural glasses from tuff grains.

No. of analyses	1		2		3		4		5		6		7		8	
	9	std †	4	std	1	3	std	1	4	std	4	std	4	std	1	
SiO ₂	48.54	0.17	48.87	0.22	51.67	55.68	0.34	52.97	54.81	0.18	55.13	0.15	54.82			
TiO ₂	1.38	0.05	1.65	0.06	0.96	1.15	0.03	1.22	1.06	0.04	1.00	0.03	1.05			
Al ₂ O ₃	15.05	0.14	13.67	0.11	15.08	15.97	0.17	15.21	15.53	0.05	15.68	0.12	15.56			
FeO*	10.35	0.11	12.46	0.17	11.89	7.30	0.36	9.63	8.15	0.05	8.01	0.07	7.96			
MgO	8.44	0.14	7.04	0.15	7.27	6.85	0.01	7.13	8.21	0.09	7.88	0.04	7.99			
CaO	12.74	0.06	11.63	0.08	8.44	9.28	0.16	9.64	8.33	0.07	8.33	0.05	8.28			
Na ₂ O	2.15	0.11	2.50	0.03	2.13	2.09	0.21	2.15	2.19	0.08	2.16	0.09	2.19			
K ₂ O	0.17	0.04	0.21	0.02	0.73	0.76	0.02	0.41	1.00	0.04	0.98	0.05	0.94			
	98.82		98.03		98.17	99.08		98.36	99.28		99.17		98.79			
Cr in ppm			180		1270	900			880		860		880			
CIPW norm																
Q					1.03	8.32		4.16	4.67		5.68		5.39			
or	1.01		1.24		4.31	4.50		2.41	5.91		5.79		5.55			
ab	18.15		21.11		18.03	17.69		18.10	18.53		18.28		18.53			
an	30.86		25.42		29.44	31.96		30.50	29.60		30.20		29.85			
di	26.27		26.55		10.32	11.50		14.56	9.57		9.09		9.15			
hy	8.24		11.96		33.22	22.95		26.32	28.99		28.24		28.32			
ol	9.64		6.23													
mt	1.98		2.39													
il	2.62		3.13		1.82	2.18		2.31	2.01		1.89		2.00			
Mg/(Mg + Fe _{total})	0.59		0.50		0.52	0.66		0.57	0.67		0.64		0.64			
norm. plag.																
An % from cation norm	61.6		53.2		60.6	63.0		61.4	60.1		60.9		60.3			

* Total iron as FeO. † One standard deviation.

Fe₂O₃/FeO ratio in norm calculation is 0.15 for 1 and 2, and 0.00 for 3 to 8.

1: Yellow basaltic glass grains, with or without olivine pseudomorphs, chromite and plagioclase. GGU 8542.

2: Yellow basaltic glass grains with plagioclase phenocrysts. GGU 5646, tuff layer 3.

3: Yellow sediment contaminated basaltic glass with native iron. GGU 5646, tuff layer 1.

4: Colourless andesite glass with graphite and phenocrysts of plagioclase and orthopyroxene. GGU 5647, tuff layer 1.

5: Very fine grained, partly glassy basaltic groundmass. The grains contain plagioclase phenocrysts. GGU 5646, tuff layer layer 7.

6: Light brown basic andesite with microphenocrysts of olivine. The glass contains graphite and native iron bearing sulphide blebs. GGU 8034.

7: Colourless andesite glass with microphenocrysts of olivine and orthopyroxene. The glass contains graphite and native iron bearing sulphide blebs. GGU 8034.

8: Colourless andesite glass with phenocrysts of orthopyroxene. GGU 8034.

often strongly vesicular. These glasses are mostly homogeneous although small scale inhomogeneities are not uncommon. Crystals of chromite (table 4 no. 5) and carbonate pseudomorphs after olivine or orthopyroxene are observed in some glasses.

In addition to basaltic glasses a large variety of more silicic glass grains are found mostly of andesitic composition. Some are extremely inhomogeneous (fig. 5), and quenching of very different melts in a state of initial mixing is clearly recorded. Some inhomogeneous andesitic grains contain graphite and disseminated native iron together with chromite and sometimes plagioclase and/or orthopyroxene. Several fairly homogeneous graphite-andesite grains (table 3 no. 4) with phenocrysts of plagioclase (An₇₂₋₇₄) and orthopyroxene (En₈₂) occur.

Crystalline fragments are widespread especially in the top of the layer. Micronoritic rocks composed of plagioclase, orthopyroxene, glassy residuum, rutile and sometimes graphite are common here. Microxenoliths and xenocrysts derived through reactions between the magma and the sediment at high temperatures are widespread, although a minor component. Light reddish magnesian spinel (table 4 no. 6), with or without graphite-bearing basic plagioclase (An₆₀₋₈₁), is most common, while green spinel, mullite and corundum are scarce.

Tuff layers 6 and 7 resemble layer 1 but are less complex. Most of the volcanic fragments are microcrystalline or semicrystalline, with a nearly opaque fine-grained groundmass (table 3 no. 5) in which plagioclase is the most common phenocryst while augite and chromite are subordinate. A few glass fragments with fresh microphenocrysts of olivine (Fo₉₀) and plagioclase are also found. Numerous glass grains with mullite needles and rare grains with euhedral red spinel (table 4 no. 7) and mullite are found. Xenocrysts of sedimentary origin, including cordierite capped by plagioclase are common. Fragments of basic plagioclase, augite and tholeiitic basalt are numerous.

Sample GGU 8034, the major tuff horizon no. 3 from Qaersutjærdalen, is typical of the olivine-microporphyrritic graphite-andesites. It is a moderately well-cemented tuff with volcanic fragments occasionally exceeding 8 mm in size. The matrix is composed of very fine-grained masses of light green to brownish sheet-silicates and silica. The volcanic components are glassy to microcrystalline andesite fragments which always show extensive alteration along the margins. The glass is light brownish to colourless and individual grains are homogeneous, although a slight inter-grain variation has been recorded (table 3 no. 6-8). A generation of olivine phenocrysts of up to 1 mm shows resorption



Fig. 5. Flow-folded, highly inhomogeneous glass, recording the initial stage of mixing of basaltic magma and liquid derived from the melting of sediment. Some of the tiny black spots are spheres of sulphide and iron, others are gas bubbles. GGU 5646, tuff layer no. 1. Analyses from this grain are shown in table 4.

and are pseudomorphosed, while a generation of euhedral microphenocryst olivine (FO_{84-85}) (table 4 no. 1) has been preserved in some glasses (fig. 6). Euhedral orthopyroxene microphenocrysts (En_{60}) are widespread. Some andesite grains carry reversely zoned orthopyroxene phenocrysts (table 4 no. 2). Graphite occurs throughout the volcanic fragments, dispersed in the groundmass of the crystalline andesites while in the glass grains it is nearly confined to the interior of vesicles. This indicates that gas evolved around the graphite grains during eruption.

Sample GGU 8542 (from the top of the tuff sequence on south side of Agatkløft in Agatdalen) exemplifies the *orthopyroxene-porphyrific graphite-andesites*. It is a carbonate-cemented rock with up to 4 mm volcanic grains which, apart from a thin palagonite rim, are very fresh-looking. The dominant fragments are colourless glassy to microcrystalline andesite, with varying degrees of vesicle formation. The glass is very homogeneous with only negligible inter-grain variation. The only phenocrysts are orthopyroxenes showing a reverse zonation from En_{80} in the cores to En_{67} in the margins, which is the typical composition of the microphenocrysts (table 4 no. 3). Graphite is widespread, showing the same type of occurrence as in the olivine graphite-andesites.

Inhomogeneous glass grains compose very little of this tuff. They show strong flow folding and pigmentation and include crystals of plagioclase and/or orthopyroxene. Their composition varies from basaltic to basic andesitic.

Another minor component is yellow basaltic glass grains some of which are rich in carbonate-pseudomorphosed olivine pheno-

crysts. Semiopaque chromite (table 4 no. 4) and microphenocrystic plagioclase (An_{74-77}) also occur in the glass. Some glasses carry plagioclase alone or are aphyric. Irrespective of crystal content the yellow glasses are of nearly identical composition (table 3 no. 1). Scattered throughout the tuff are red magnesian spinels and graphite-bearing plagioclase xenocrysts.

Chemistry of the glasses

Yellow basaltic glasses (GGU 8542) with chromite, olivine pseudomorphs and plagioclase are similar to phenocryst-poor tholeiitic basalts and glasses in picritic pillows from the Vaigat Formation (VF) and plot within the field of the Vaigat Formation basalt while plagioclase-porphyrific yellow glass (GGU 5646, tuff layer no. 3) is slightly more evolved and similar to the Vaigat Formation plagioclase-porphyrific basalts (fig. 7). Both types of yellow glass are olivine-normative tholeiitic basalts resembling MORB glasses. Representative analyses of glasses considered only slightly hydrated are presented in table 3.



Fig. 6. Graphite-andesite glass with an euhedral phenocryst of olivine (top) and an immiscible sulphide-metallic iron sphere (bottom) similar to that shown in fig. 10. A few flakes in the glass are graphite. GGU 8034.

Table 4. Chemical analyses of phenocrysts and xenocrysts.

	1	2	3	4	5	6	7
	Olivine	Orthopx	Orthopx	Chromite	Chromite	Spinel	Spinel
SiO ₂	39.73	53.54	55.25	0.28	0.09	n.d.	n.d.
TiO ₂	n.d.	n.d.	n.d.	0.96	0.99	n.d.	0.23
Al ₂ O ₃	n.d.	3.65	2.02	24.36	23.39	66.55	62.34
Cr ₂ O ₃	n.d.	0.71	0.61	36.03	43.14	n.d.	0.25
V ₂ O ₅	n.d.	n.a.	n.a.	n.d.	1.54*	0.08	n.d.
Fe ₂ O ₃	n.a.	n.a.	n.a.	9.13	1.50	n.a.	n.a.
FeO	14.01	11.44	8.55	15.82	17.08	16.47	28.40
MnO	n.d.	n.d.	0.12	0.31	n.d.	n.d.	n.d.
MgO	45.60	29.57	31.71	13.60	12.62	17.03	8.75
CaO	0.12	0.45	1.14	0.26	0.17	n.d.	n.d.
	99.46	99.36	99.40	100.75	100.52	100.13	99.97
Calc. basis	4(0)	6(0)	6(0)	Δ24 cat/ 32(0)	Δ24 cat/ 32(0)	32(0)	32(0)
Si	0.998	1.906	1.944	0.068	0.022		
Ti				0.175	0.181		0.037
Al		0.153	0.084	6.954	6.715	15.998	15.926
Cr		0.020	0.017	0.175	8.305		0.043
V					0.300	0.013	
Fe ^{III}				1.663	0.274		
Fe ^{II}	0.294	0.341	0.252	3.204	3.579	2.809	5.147
Mn			0.004	0.064			
Mg	1.707	1.569	1.663	4.908	4.580	5.175	2.826
Ca	0.003	0.017	0.043	0.067	0.044		
cation sum	3.002	4.007	4.006	24.000	24.000	23.995	23.978
100 Mg/(Mg + Fe ²⁺)	85.3	82.2	86.9	60.5	56.1	64.8	35.4

Δ Ferric iron calculated by assuming stoichiometry (Finger 1972)

* Wavelength dispersive analysis.

n.d. not detected. n.a. not analysed.

1: Olivine microphenocrysts in graphic-andesite glass. GGU 8034.

2: Core of orthopyroxene phenocrysts in graphite-andesite glass. GGU 8034.

3: Orthopyroxene microphenocrysts in andesite glass. GGU 8542.

4: Chromite in yellow basaltic glass with olivine pseudomorphs. GGU 8542.

5: Chromite in sediment contaminated basalt glass. GGU 5646, tuff layer 1.

6: Slightly reddish spinel in xenolithic plagioclase-graphite-spinel rock. GGU 5646, tuff layer 1.

7: Euhedral dark red spinel in alumina-rich glass with mullite. GGU 5646, tuff layer 1.

The sediment-contaminated glasses deviate strongly from the VF basalt field. They are moderately to strongly enriched in SiO₂ and Al₂O₃ but depleted in CaO (fig. 7). Enrichment in K₂O was also noted. At comparable MgO levels the glasses are to a varying degree depleted in FeO (fig. 7a). The glasses are unusually Cr rich (table 3), the only comparable glasses on earth being from the highly reduced sediment-contaminated volcanics from Disko and Precambrian komatiite glasses in their inferred original unaltered condition (Green et al. 1975).

In terms of normative mineralogy (fig. 8) the yellow glasses plot around the olivine-poor end of the Vaigat Formation olivine control line in the normative hypersthene space. The magmas affected by sediments deviate from this trend by

their much lower diopside component and the presence of normative quartz, even when total iron is calculated as FeO.

Two stages in the magma-sediment reactions have been preserved by the eruptive quenching. The first stage is represented by GGU 5646, tuff layer no. 1, where quartz-normative Ca-depleted basalt compositions are found together with inhomogeneous glasses ranging from basaltic to nearly plagioclase-glass compositions within a single grain. High degrees of melting of non-volcanic materials are clearly displayed in an initial stage of mixing with basalt. The inhomogeneous graphite-bearing andesite grains with native iron represent a more advanced stage of contamination where strong variations in FeO, MgO and CaO contents show that disequilibrium down to the scale of a

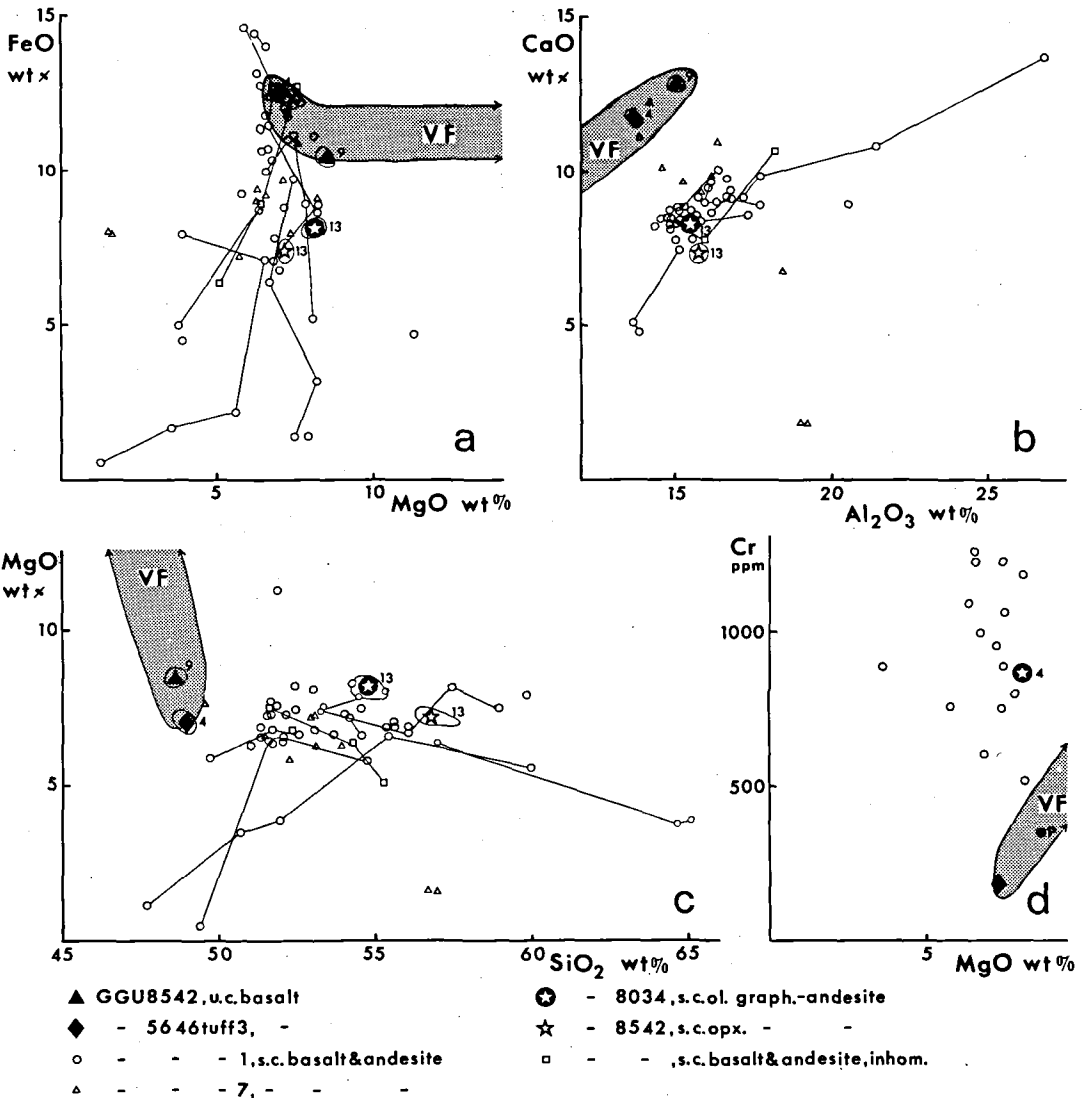


Fig. 7. Glass analyses from the Abraham Member. The shaded area shows the variation in the basalts from the Vaigat Formation (VF) on northern Disko. Filled symbols denote uncontaminated (u.c.) and open symbols sediment-contaminated (s.c.) basaltic compositions. The large symbols indicate compositions of homogeneous glass types, encircled to show scatter, and with numbers indicating the number of analysed points. Thin lines connect analysed glass points from within inhomogeneous glass grains. Note that the uncontaminated basalt glasses plot within the field of the Vaigat Formation basalts. In fig. 7c note the unusual combination of high magnesia and silica, exemplified by

the olivine-graphite-andesites (GGU 8034) and the orthopyroxene-graphite-andesites (GGU 8542). The sediment-contaminated glasses are characterized by lower Ca/Al ratios than the uncontaminated glasses (fig. 7b). Note the presence of high-alumina glasses derived from sediments. In fig. 7d P shows the composition of glass in a picritic pillow from northern Disko. The unusually high Cr contents in the contaminated glasses were caused by prevailing low oxygen fugacities, preventing chromite precipitation at the time of quenching, and show that the parent magmas were highly magnesian picrites.

few microns was still present. However, the high Cr contents of the glasses and the commonly included chromite grains show that the predominant melt component of these grains was basaltic.

The second stage is represented by the olivine-graphite-andesites (GGU 8054) and the orthopyroxene-graphite-andesites (GGU 8542). Here a considerable homogenization of the sediment-con-

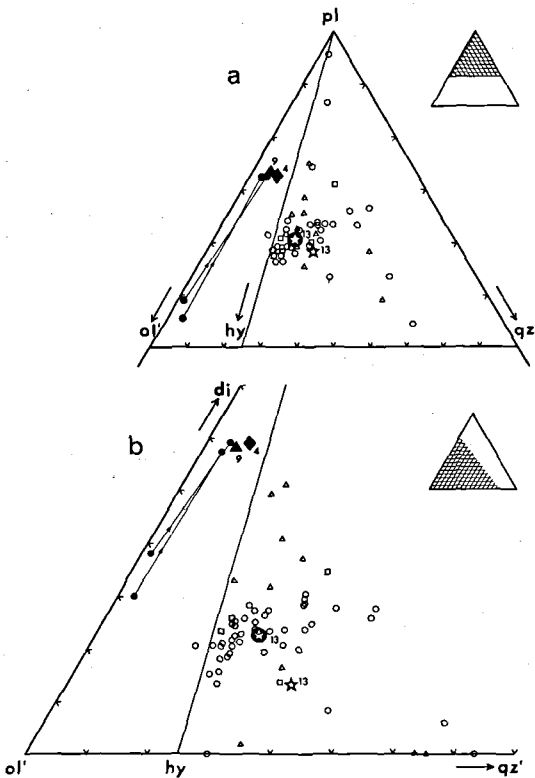


Fig. 8. Glass analyses from the Abraham Member. Cation-normative ternary plots. Filled circle pairs with arrows show picrites from the Vaigat Formation connected with their quench glasses. Otherwise symbols as in fig. 7. Norms are calculated with $Fe_2O_3/FeO = 0.15$ in uncontaminated rocks and glasses, and 0.0 in sediment-contaminated glasses. In 8a note the higher hy/pl ratio in most sediment-contaminated glasses compared to the uncontaminated glasses. In 8b note the similarity between uncontaminated basalt glasses and Vaigat Formation picrite glass. In comparison, note the much lower normative di in sediment-contaminated andesites. Some glasses with a high sediment component are corundum-normative. Only compositions with $ol' + qz' + di > 25\%$ are shown.

taminated melts is recorded by the small standard deviations shown by analyses on many andesite glass grains. A similar substantial homogenization has been observed in contaminated iron-bearing andesite lavas on Disko where many cubic kilometres of fairly homogeneous, strongly contaminated andesite were sometimes the product of a single eruption (Pedersen 1977). The homogenized andesites must be characterized as subalkaline high-magnesium andesites. They are of an unusual type, but are found as sediment-contaminated highly reduced andesites in the Vaigat Formation on

Disko. The closest analogues found outside West Greenland are probably high-magnesium andesites from western Papua New Guinea (Mackenzie 1976) or from the western Sunda Arc (Nicholls & Whitford 1976); however these rocks are much more alkaline and with a different genesis.

Sulphides and metallic iron

High-temperature sulphides and iron metal have only been preserved in well cemented samples. That such phases have survived at all in Tertiary tuffs, deposited in saline water, is surprising. The following description deals only with magmatic sulphides and iron from the three tuff samples that have already been described petrographically. (A brief of the diagenetic opaque phases in GGU 5646, tuff layer no. 1, indicates complex and unusual parageneses including a Fe and Cu bearing NiS phase, heazlewoodite, Co and Cu bearing violarites, siegenite, chalcopyrite, pyrite and Ni-Cu-alloy. Detailed descriptions will be presented elsewhere).

GGU 5646, tuff layer no. 1, contains scarce magmatic sulphides and iron occurring as small (less than 15 microns) spheres with a metal-rich core and a troilite mantle (fig. 9). Detailed metal textures have not been resolved due to the tiny size of the spheres, but their gross structure resembles the iron-troilite bodies described in detail by Pauly (1969) from Asuk on Disko. In the inhomogeneous graphite-andesite grains the iron-troilite spheres are finely disseminated in the glass and never exceed a few microns in size; therefore no analyses could be obtained. In the olivine-graphite-andesite (GGU 8034) nearly unaltered spherical or ellipsoidal sulphide bodies (figs 6,10) are preserved in some glass grains, whereas they are partly or completely decomposed in the microcrystalline andesite fragments. The sulphide bodies occasionally exceed 50 microns in size. They consist of iron monosulphide, pentlandite, a Cu-rich phase, and a very minor, highly reflecting phase only up to 2 microns in size, rich in Fe and Ni, which is identified as native iron. No oxide phase is observed in the sulphide bodies but Cr has an inhomogeneous distribution, probably caused by submicroscopic chromites exsolved from the sulphides. Representative modal analyses of sulphide blebs obtained from grid-counting of enlarged high-magnification photographs (table 6 no. 5-7) show consistency with bulk chemical analyses of the blebs (table 5 no. 5-7).

In the orthopyroxene-graphite-andesite (GGU 8542) sulphide blebs are found similar to those in the olivine-graphite-andesite (GGU 8034), also here only well preserved when included in glass. Occasionally a size of up to 125 microns has been observed, but only blebs less than 40 microns in size have preserved parts of a very minor iron metal phase. Compared to the olivine-graphite-andesite, the blebs have mostly a slightly coarser texture (fig. 11) indicating a slightly longer cooling time. A few modal analyses (table 6 no. 1, 2 and 4) and bulk chemical analyses (table 5 no. 1, 2 and 4) are given.

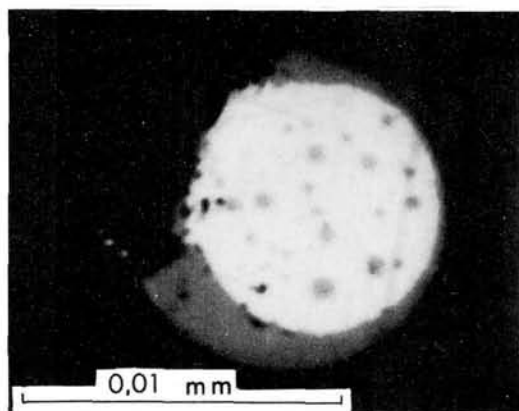


Fig. 9. A tiny sphere consisting of a mantle of iron monosulphide and a core of metallic iron. The core contains very small spheres of iron monosulphide. The body is enclosed in yellow basaltic glass. GGU 5646, tuff layer no. 1. An analysis of the core is shown in table 5, col. 8.

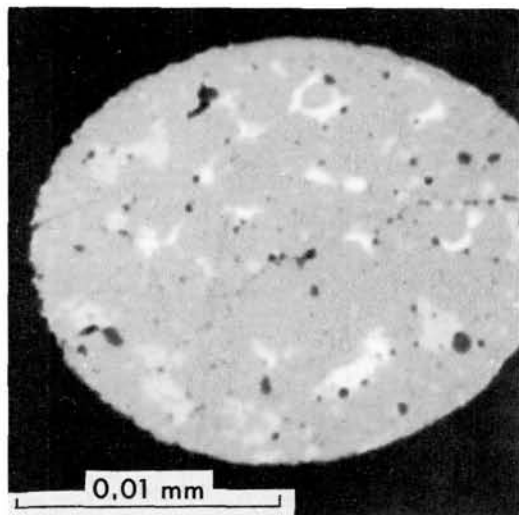


Fig. 10. A spheroidal body of iron monosulphide (grey), pentlandite + Cu-rich phases (lighter grey) and iron (white). An immiscible, quenched sulphide melt now enclosed in olivine-graphite-andesite glass. GGU 8034. Chemical analysis in table 5, col. 5.

Chemistry of the sulphide blebs

A single iron-core from the iron-troilite spheres in sample GGU 5646, tuff layer no. 1, was analysed and shown in table 5 no. 8. It contains a substantial schreibersite (Fe_3P) component, and high S which is caused by tiny troilite spheres in the iron.

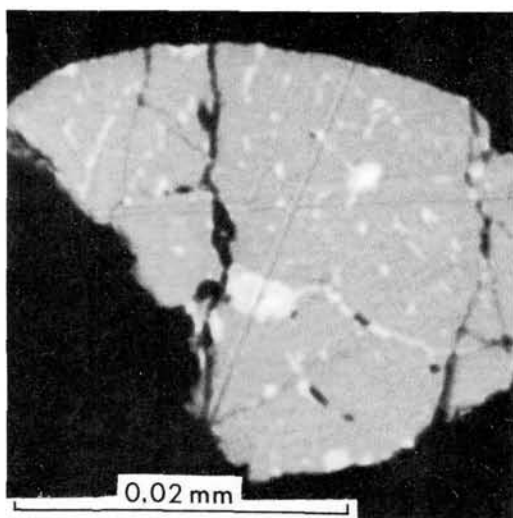


Fig. 11. Fairly coarse-textured small body of iron monosulphide (grey), pentlandite + Cu-rich phases (lighter grey) and iron (white). The pentlandite + the Cu-rich phases form caps around the iron and small veins between and inside the troilitic iron monosulphide grains. Immiscible sulphide-iron bleb enclosed in orthopyroxene-graphite-andesite glass. GGU 8542. Chemical analyses are shown in table 5, cols. 4, and modal analysis in table 6.

Other iron-cores are poor in P, and no generalizations can be made. The chemical composition of sulphide blebs in the graphite-andesites (GGU 8034 and 8542) closely approximates the Fe-Ni-S-system (table 6). Next in abundance are Cu and Co while P has not been detected. Cr is present in small but analytically significant amounts. The $\text{Cu}/(\text{Cu} + \text{Ni})$ atomic ratios vary from 0.07–0.26 and are typical for sulphide melts equilibrated with very magnesian magmas (e.g. Naldrett & Cabri 1976 and Czamanske & Moore 1977) and the observed ratios can be interpreted as an inheritance from a Ni-rich picritic parent. However, the total content of Ni + Cu + Co is unusually low for immiscible sulphide melts from basic magmas (e.g. compare with Mathes & Yeats 1976 and Czamanske & Moore 1977) and is a strong indication that sedimentary sulphur was assimilated into the Nûgssuaq magmas causing a dilution of the highly chalcophile minor elements in the immiscible sulphide melts. With their low content of Ni + Cu + Co, their small content of a metallic phase and the absence of notable oxides, the sulphide blebs form a hitherto unrecorded type of immiscible sulphide-rich melt.

Table 5. Chemical analyses of sulphides and iron (wt. %).

	1	2	3	4	5	6	7	8
Fe	59.05	60.50	59.52	59.52	60.35	59.58	58.10	85.10
Ni	2.90	5.07	4.50	3.62	5.52	4.99	4.88	3.03
Cu	1.08	0.95	0.95	0.31	0.88	0.52	0.85	0.81
Co	0.26	0.33	0.23	0.19	0.30	0.28	0.28	0.58
Cr	0.11	0.14	0.12	0.05	0.13	0.11	0.13	0.01
S	33.91	33.46	33.56	35.00	32.04	31.83	33.40	2.75
P	< 0.01	< 0.01	< 0.01	< 0.01	< 0.01	< 0.01	< 0.01	2.61
	97.32	100.46	98.89	98.70	99.23	97.32	97.65	94.89
Atomic ratio (Fe + Ni + Cu + Co)/S	1.066	1.140	1.109	1.040	1.194	1.173	1.096	
Atomic ratio Cu/(Cu + Ni)	0.26	0.15	0.16	0.07	0.13	0.09	0.14	0.20
Size in microns of analysed bleb	30	25	20	26	32	24	17	9.5

- 1: Sulphide bleb, fairly coarse in texture, included in orthopyroxene graphite-andesite glass. GGU 8542.
- 2: Sulphide bleb included in orthopyroxene graphite-andesite glass. GGU 8542.
- 3: Sulphide bleb included in orthopyroxene graphite-andesite glass. GGU 8542.
- 4: Sulphide bleb (fig. 11) included in orthopyroxene graphite-andesite. GGU 8542.

- 5: Sulphide bleb in olivine graphite-andesite glass (fig. 10). GGU 8034.
- 6: Sulphide bleb in olivine graphite-andesite glass. GGU 8034.
- 7: Sulphide bleb in olivine graphite-andesite glass. GGU 8034.
- 8: Spheroidal iron metal with tiny iron sulphide spheres. The iron is capped by iron monosulphide (fig. 9). GGU 5646, tuff layer 1.

Table 6. Modal analyses of chemically analysed immiscible sulphide blebs (vol. %).

Analysis no in table 5	1	2	4	5	6	7
Iron monosulphide	92	93	94	89	90	89
Pentlandite + Cu rich phase	4.7	3.0	4.9	8.3	7.5	9.1
Iron metal*	0.7	1.5	0.2	0.7	1.9	0.5
Scratches and holes	2.4	2.3	0.3	1.8	1.1	1.4

* Iron, cohenite and schreibersite.

Table 7. Mineral - glass thermometry.

GGU sample no.	Glass type	Method	Temperature °C	K _D *
Uncontaminated rock types				
5646, tuff 3	basalt + plag	A	1204, 1216, 1218	
8542	basalt + plag + ol pseud + chr	A	1198	
8542	basalt + plag	A	1212	
Sediment contaminated rock types				
8034	graphite-andesite + ol + opx	B ₁	1198	0.30
		B ₂	1213	
8034	graphite-andesite + ol + opx	B ₁	1208	0.31
		B ₂	1208	
8542	inhomog. andesite + plag + opx	A	1164	
5646, tuff 1	basalt + plag	A	1151	
5646, tuff 1	basic andesite + plag + iron	A	1167	
5646, tuff 1	graphite-andesite + plag + opx	A	1176	
5646, tuff 7	basic andesite + plag + ol	B ₁	1166	0.31
		B ₂	1165	
5646, tuff 7	basalt matrix + plag	A	1184	
5646, tuff 7	Al ₂ O ₃ -rich glass + plag	A	1135	

A: Plagioclase-glass thermometry, Mathez (1973, equation 7 a). P_{H₂O} = 1 bar assumed.

B₁: Olivine-glass thermometry, Roeder (1974, equation 4).

B₂: Olivine-glass thermometry, Roeder (1974, equation 5).

*: Fe₂O₃/FeO is assumed to be 0.

$$K_D = X_{FeO}^{ol} / X_{MgO}^{ol} \cdot X_{MgO}^{liq} / X_{FeO}^{liq}$$

plag = plagioclase, ol = olivine, chr = chromite, opx = orthopyroxene.

Interpretation and discussion

Thermometry

In order to place some constraints on the magmatic evolution two empirically calibrated crystal-glass thermometers have been applied to glass grains containing either olivine, plagioclase or both. The results, summarized in table 7, rest heavily on the assumption that the glasses are unaltered.

The olivine-glass thermometer of Roeder & Emslie (1970) as updated by Roeder (1974) was applied to the few glasses with microphenocrystic olivine. K_D values (table 7) indicating equilibrium are found for olivine-glass pairs when all iron in the glasses is calculated as FeO, an expression of the reduced state of the rocks.

The Kudo-Weill plagioclase-glass thermometer as modified by Mathez (1973) has been applied to numerous plagioclase-glass pairs. A water pressure

of 1 bar is assumed in the calculations, clearly a minimum for explosive eruptions.

The uncontaminated yellow basaltic glasses give quench temperatures of 1200–1220°C, which is similar to temperatures obtained by the same methods from the Vaigat Formation picrite pillows from Disko. Olivine-graphite-andesites quenched in the range 1200–1215°C while some contaminated basalts and the other andesites seemingly quenched in the temperature range 1135–1185°C. The quench temperatures of the olivine-graphite-andesite give support to the textural interpretation that the sulphide blebs in these glasses were entirely liquid prior to the quenching. It seems justified to assume that the bulk of the magmas of the Abraham Member equilibrated around 1200°C, and that some magmas had temperatures down to 1150°C.

Parent magma compositions

The Cretaceous to Tertiary sediments in the Disko-Nûgssuaq region contain less than 200 ppm Cr, and it can be concluded that high Cr contents in the sediment-contaminated glasses were inherited from the parent magmas. If Vaigat Formation type parent magmas are assumed, the MgO content of the parent magmas can be estimated from the Cr-Mg ratio (fig. 7d). With about 1200 ppm Cr in some sediment-contaminated glasses (which may carry chromite microphenocrysts in addition) a minimum content of 17–18 per cent MgO is estimated. (Measured olivine-glass partition coefficients for Cr in Disko picrite glass and in olivine-graphite-andesite (GGU 8034) are close to unity). Allowing for some Cr to have precipitated as chromite or orthopyroxene and for the dilution effect of the sediment-contamination, a parent magma (melt + crystals) with a MgO content of above 20 weight per cent is indicated. It is therefore concluded that the parent magmas were highly magnesian tholeiitic picrite basalts. This is further supported by the picrite Ni-Cu-Co ratios found in the immiscible sulphide blebs in the graphite-andesites.

Fe-metal/FeO ratios

The iron-bearing graphite-andesites from the Abraham Member have a composition very similar to several iron-bearing andesites from the Vaigat Formation on Disko, but deviate from the

latter by their much lower Fe-metal/FeO ratios. This could be due either to metal fractionation or to a difference in state of oxidation.

Some Abraham Member graphite-andesites contain reversely zoned orthopyroxene phenocrysts which indicate that the Mg/(Mg + Fe²⁺) ratios increased in these magmas during the pyroxene crystallization prior to the eruptions. This increase was almost certainly caused by removal of iron from the silicate melt into either Fe-metal or FeS. Iron and sulphides, when segregated in larger than very minute bodies, are subject to strong gravitational fractionation in a magma, provided the viscosity is low, and to extreme aeolian fractionation. However, the Abraham Member graphite-andesites have only a few weight per cent less FeO_{total} than their Vaigat Formation type picritic parents (fig. 7), and it can therefore be concluded that they have at most lost a few weight per cent of iron through metal or sulphide fractionation. The difference in the Fe-metal/FeO ratios must therefore reflect equilibration under low but different oxygen fugacities. A simple explanation may be found in the eruption mechanisms. Graphite-oxygen equilibria are strongly pressure dependent in the pressure range 1 bar to 1 kbar, pressure increase leading to increased oxygen fugacities (French & Eugster 1965, French 1966). Neglecting the other gas-components (graphite-oxygen do not form an oxygen buffer in a natural multicomponent gas system) an explosive quenching of a magma from a moderate pressure regime (e.g. 0.5–1 kbar) will reflect a higher f_{O_2} (as exemplified by the Abraham Member graphite-andesites) than a slow upflow followed by low pressure equilibration of the same magma (as exemplified by native iron bearing andesites from Disko).

Summary and conclusions

The Abraham Member tuffs contain a detailed volcanic record which, despite the present fragmentary knowledge, allows some general interpretations. The compositional range and volume proportions of the rock types show a dominance of olivine-graphite-andesites and orthopyroxene-graphite-andesites, while rock types similar to the uncontaminated – tholeiitic basalts from the overlying Vaigat Formation are very subordinate. This scarcity of uncontaminated tuff material does not

imply that such eruptions were rare at the time of deposition of the Abraham Member, but that these eruptions were largely effusive and that their eruption products were not spread as far as the Agatdal area. So, the Abraham Member tuffs represent mainly the magmas which became gas-enriched prior to eruption through reaction with sediments.

The formation of the Abraham Member tuffs can thus be summarized. At a time when regional picritic lavas and hyaloclastites of the Vaigat Formation volcanism were gradually transgressing older and contemporary sedimentary basins, very magnesian picritic magmas were trapped in high-level magma chambers in carbon-rich sedimentary strata which overlie the Precambrian basement. The magmas reacted with the sediments at temperatures around or slightly above 1200°C and at pressures of less than 1 kbar (geophysical evidence (Elder 1975) indicates that the sediments in central Nûgssuaq are no more than 3 km thick) and became gas-enriched from volatile sedimentary components. This led to a large number of explosive eruptions which spread graphite-andesite ash into areas which had not earlier received volcanic deposits. The length of the time interval spanned by the tuffs is not known. The very short time exposed to sea-water before effective chemical sealing of the individual tuffs was achieved, together with the overall homogeneity of the tuff sequence, indicates a rather short duration.

The Abraham Member tuffs thus seem to constitute a new major occurrence of iron-bearing basalts and andesites. In the number of recorded iron-bearing eruptions it exceeds the activity from all other known centres with native iron volcanism in the early epoch spanned by the Vaigat Formation volcanism and draws attention to central and eastern Nûgssuaq as a potentially important centre for an unusual volcanism.

Appendix: methods

Chemical analyses of glasses, silicates, oxides, sulphides and metals were obtained by microprobe analysis. Most of the work on glasses, silicates and oxides was made with TPD microprobe at the Research School of Earth Sciences, Canberra, with an energy-dispersive analysis system described by Reed & Ware (1975). The probe is operated at 15 kV and with a sample current of 5 nA as measured in a Faraday cage. A few analyses of Cr in glasses were made using a semifocussing crystal spectrometer at 20 kV and with a sample current of 50 nA.

A few analyses of glasses, silicates and oxides were obtained at the Grant Institute of Geology, Edinburgh, with a Microscan 5 microprobe operated at 20 kV and with a sample current of 30 nA as measured in a Faraday cage.

Analyses of sulphides and metals were made at Institute of Mineralogy, University of Copenhagen, with a Hitachi XMA 5B Scanning Electron Microanalyser operated at 20 kV and with a sample current of 25 nA as measured in a Faraday cage. Synthetic sulphide standards supplied by S. Kissin were applied together with metals.

Quantitative matrix correction was applied to all results.

Acknowledgements. The author is grateful to P.G. Hill, J.G. Rønsbo and N.G. Ware for technical assistance with the microprobe work, to the Research School of Earth Sciences, Australian National University, Canberra, and the Danish Natural Science Research Council, for providing laboratory facilities; to L.M. Larsen for criticism of the manuscript, and to N. Hald, F. Ulf-Møller and S. Watt for editorial assistance. The publication was authorized by the Director of the Geological Survey of Greenland.

Dansk sammendrag

Tuffer fra Agatdal Formationen på det centrale Nûgssuaq Vestgrønland, består overvejende af olivin-grafit-andesit og orthopyroxen-grafit-andesit, mens bjergarter, der i sammensætning svarer til de overliggende magnesium-rige, tholeiitiske basalt-lavaer fra Vaigat Formationen, er mindre almindelige. Det antages, at de grafitførende andesiter er dannet som følge af en reaktion mellem magnesium-rige basaltmelter og kulstofholdige sedimenter i højtliggende magmakamre ved temperaturer omkring eller lidt over 1200°. Ved reaktionen fik smelterne bl.a. tilført gasser, hvilket resulterede i eksplosive udbrud. Tufferne glaskorn er sædvanligvis velbevarede og nogle tuffer indeholder små lynafkølede sulfidlegemer med metallisk jern. De grafitførende, andesitiske tuffer svarer i sammensætning til visse intermedizære lavaer med metallisk jern, der forekommer i Vaigat Formationen på Disko, og som formodes at være kommet til udbrud omtrent samtidig med tufferne.

References

- Clarke, D.B. & Pedersen, A.K. 1976: Tertiary volcanic province of West Greenland. In Escher, A. & Watt, W.S. (edit.) *Geology of Greenland* 364–385. Copenhagen: Geological Survey of Greenland.
- Czamanske, G.K. & Moore, J.G. 1977: Composition and phase chemistry of sulfide globules in basalt from the Mid-Atlantic Ridge rift valley near 37° N lat. *Geol. Soc. Amer. Bull.* 88: 587–599.
- Elder, J.W. 1975: A seismic and gravity study of the western part of the Cretaceous – Tertiary sedimentary basin of central West Greenland. *Rapp. Grønlands geol. Unders.* 69: 5–9.
- Finger, L.W. 1972: The uncertainty in the calculated ferric iron content of a microprobe analysis. *Carnegie Instn. Wash. Yb.* 71: 600–603.
- Floris, S. 1972: Scleractinian corals from the upper Cretaceous and lower Tertiary of Nûgssuaq, West Greenland. *Bull. Grønlands geol. Unders.* 100 (also *Meddr Grønland* 196,1) 132 pp.
- French, B.M. 1966: Some geological implications of equilibrium between graphite and a C – H – O gas phase at high temperatures and pressures. *Rev. Geophys.* 5: 223–253.
- French, B.M. & Eugster, H.P. 1965: Experimental control of oxygen fugacities by graphite – gas equilibria. *J. Geophys. Res.* 70: 1529–1539.

- Green, D.H., Nicholls, I.A., Viljoen, M. & Viljoen, R. 1975: Experimental demonstration of the existence of peridotitic liquids in earliest Archaean magmatism. *Geology*, 3: 11-14.
- Hald, N. 1977: Normally magnetized lower Tertiary lavas on Nûgssuaq, central West Greenland. *Rapp. Grønlands geol. Unders.* 79: 5-7.
- Hansen, H.J. 1970: Danian foraminifera from Nûgssuaq, West Greenland, with special reference to species occurring in Denmark. *Bull. Grønlands geol. Unders.* 93 (also *Meddr Grønland* 193,2) 132 pp.
- Hart, S.R., Erlank, A.J. & Kable, E.J.D. 1974: Sea-floor basalt alteration: some chemical and Sr isotopic effects. *Contr. Mineral. Petrol.* 44: 219-230.
- Hekinian, R. & Hoffer, M. 1975: Rate of palagonitization and manganese coating on basaltic rocks from the rift valley in the Atlantic ocean near 36°50' N. *Marine Geology*, 19: 91-109.
- Henderson, G., Rosenkrantz, A. & Schiener, E.J. 1976: Cretaceous - Tertiary sedimentary rocks of West Greenland. In Escher, A. & Watt, W.S. (edit.) *Geology of Greenland*, 340-362. Copenhagen: Geological Survey and Greenland.
- Koch, B.E. 1959: Contribution to the stratigraphy of the non-marine Tertiary deposits on the south coast of the Nûgssuaq peninsula, northwest Greenland, with remarks on the fossil flora. *Bull. Grønlands geol. Unders.* 22 (also *Meddr Grønland* 162,1) 100 pp.
- Koch, B.E. 1963: Fossil plants from the lower Paleocene of the Agatdalen (Angmártussut) area, central Nûgssuaq peninsula, northwest Greenland. *Bull. Grønlands geol. Unders.* 38 (also *Meddr Grønland* 172,5) 120 pp.
- Mackenzie, D.E. 1976: Nature and origin of late Cainozoic volcanoes in western Papua New Guinea. In Johnson, R.W. (edit.) *Volcanism in Australasia* 221-238. Amsterdam: Elsevier.
- Mathez, E. A. 1973: Refinement of the Kudo-Weill plagioclase thermometer and its application to basaltic rocks. *Contr. Mineral. Petrol.* 41: 61-72.
- Mathez, E.A. & Yeats, R.S. 1976: Magmatic sulfides in basalt glass from DSDP Hole 319A and Site 320, Nazca Plate. In: *Initial Reports of the Deep Sea Drilling Project* 34: 363-374. Washington: U.S. Government Printing Office.
- Munck, S. & Noe-Nygaard, A. 1957: Age determination of the various stages of the Tertiary volcanism in the West Greenland basalt province. *20th int. geol. Congr., Mexico, 1956.* 1: 247-256.
- Naldrett, A.J. & Cabri, L.J. 1976: Ultramafic and related mafic rocks: their classification and genesis with special reference to the concentration of nickel sulfides and platinum-group elements. *Econ. Geol.* 71: 1131-1158.
- Nicholls, I. A. & Whitford, D.J. 1976: Primary magmas associated with Quaternary volcanism in the western Sunda Arc, Indonesia. In Johnson R.W. (edit.) *Volcanism in Australasia* 77-90. Amsterdam: Elsevier.
- Nordenskiöld, A.E. 1871: Redogörelse för en Expedition till Grönland aar 1870. *Öfvers. Vetensk. Akad. Förh.* 27: 973-1082.
- Pauly, H. 1969: White cast iron with cohenite, schreibersite and sulphides from Tertiary basalts on Disko, Greenland. *Meddr dansk geol. Foren.* 19: 8-26.
- Pedersen, A.K. 1973: Report on field work along the north coast of Disko. *Rapp. Grønlands geol. Unders.* 53: 21-27.
- Pedersen, A.K. 1977: Tertiary volcanic geology of the Mellemfjord area, south-west Disko. *Rapp. Grønlands geol. Unders.* 81: 33-49.
- Phalen, W.C. 1903: Notes on the rocks of Nugsuaks peninsula and its environs, Greenland. *Smiths. Misc. Coll.* 45: 183-212.
- Reed, S.J.B. & Ware, N.G. 1975: Quantitative electron microprobe analysis of silicates using energy-dispersive X-ray spectrometry. *J. Petrology*, 16: 499-519.
- Roeder, P.L. 1974: Activity of iron and olivine solubility in basaltic liquids. *Earth Planet. Sci. Lett.* 23: 397-410.
- Roeder, P.L. & Emslie, R.F. 1970: Olivine - liquid equilibrium. *Contr. Mineral. Petrol.* 29: 275-289.
- Rosenkrantz, A. 1951: Oversigt over Kridt- og Tertiærformationens stratigrafiske forhold i Vestgrønland. *Meddr dansk geol. Foren.* 12: 155-158.
- Rosenkrantz, A. 1955: Vidnesbyrd om vulkansk aktivitet i Grønlands og Danmarks danien. *Meddr dansk geol. Foren.* 12: 669-670.
- Rosenkrantz, A. 1970: Marine upper Cretaceous and lowermost Tertiary deposits in west Greenland. *Meddr dansk geol. Foren.* 19: 406-453.
- Rosenkrantz, A. & Pulvertaft, T.C.R. 1969: Cretaceous - Tertiary stratigraphy and tectonics in northern West Greenland. *Mem. Amer. Ass. Petrol. Geol.* 12: 883-898.
- Scarfe, C.M. & Smith, D.G.W. 1977: Secondary minerals in some basaltic rocks from DSDP leg 37. *Can. J. Earth Sci.* 14: 903-910.
- Steenstrup, K.J.V. 1875: Om de Nordenskiöldske Jærnmasser og om Forekomsten af gedigent Jærn i Basalt. *Vidensk. Meddr naturh. Foren., København.* 16-19: 284-306.
- Steenstrup, K.J.V. 1882: Om forekomsten af Nikkeljærn med Widmanstättenske Figurer i Basalten i Nordgrønland. *Meddr Grønland*, 4: 113-132.
- Thompson, G. 1973: A geochemical study of the low-temperature interaction of sea-water and oceanic igneous rocks. *EOS* 54: 1015-1018.
- White, D. & Schuchert, C. 1898: Cretaceous series of the west coast of Greenland. *Bull. geol. Soc. Amer.* 9: 343-368.